International Journal of Machine Tools & Manufacture 150 (2020) 103517

Contents lists available at ScienceDirect

International Journal of Machine Tools and Manufacture

journal homepage: http://www.elsevier.com/locate/ijmactool

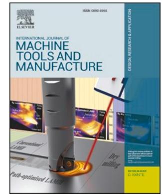

A generic approach of polishing metals via isotropic electrochemical etching

Rong Yi [a], Yi Zhang [a,b], Xinquan Zhang [c], Fengzhou Fang [d], Hui Deng [a,*]

[a] *Department of Mechanical and Energy Engineering, Southern University of Science and Technology, No. 1088, Xueyuan Road, Shenzhen, Guangdong, 518055, China*
[b] *Engineering, Faculty of Science, University of East Anglia, Norwich Research Park, Norwich, NR4 7TJ, UK*
[c] *School of Mechanical Engineering, Shanghai Jiao Tong University, No. 800, Dongchuan Road, Minhang District, Shanghai, 200240, China*
[d] *State Key Laboratory of Precision Measuring Technology & Instruments, Centre of Micro-Nano Manufacturing Technology, Tianjin University, Tianjin, 300072, China*

A R T I C L E I N F O

Keywords:
Metal materials
Polishing
Electrochemical etching
Etching anisotropy

A B S T R A C T

Isotropic etching polishing (IEP), which is based on the merging of hemispherical holes that are formed by isotropic etching, is proposed in this study as a universal metal finishing approach. Modeling of the surface evolution during IEP is also carried out, and the formation of a metal surface is predicted. The etching anisotropy of titanium is experimentally studied, and the results show that isotropic etching can be realized under optimized conditions. Isotropic etching sites originate from a breakdown of the passivation layer. Both the density and growth rate of the holes are affected by the current, and a large etching current is preferred for the realization of highly efficient polishing. IEP has been shown to be effective and efficient for surface finishing of TA2. The surface *Sa* roughness is drastically reduced from 64.1 nm to 1.2 nm, and a maximum polishing rate of 15 μm/min is achieved under an etching current of 3 A. IEP has also been successfully applied for surface finishing of other metals, including TC4, stainless steel 304, aluminum alloy 6063 and pure nickel, demonstrating that IEP can be considered a universal approach for finishing metals.

1. Introduction

Although metal components with different surface finishes have various applications for different functional requirements, improving roughness through surface finishing is still indispensable in most cases. Therefore, a surface finishing technique for metal parts must be mirror-like, cost effective and most importantly shape independent [1–3]. With the development of material science, the manufacturing technologies for metal parts has rapidly improved. Therefore, the development of metal finishing techniques has been greatly promoted [4–6].

Mechanical polishing (MP) is a widely used finishing technique, that removes the raised parts of the surface by mechanical action between the abrasives and metal surface [7,8]. As the surface material is removed or deformed by shearing or plastic deformation, MP inevitably introduces scratches, sub-surface damages (SSDs) and residual stresses in the layer [9]. Accordingly, the application of MP is limited only to rough finishing stages. To avoid SSDs, chemical-mechanical polishing (CMP), which combines a chemical surface modification followed by mechanical removal, has been utilized [10]. The surface material chemically reacts with the oxidants in the slurry and generates a relatively soft layer. Later, the mechanical action of the abrasive and the polishing pad removes the chemically developed soft layer from the surface. A fine surface finish on the workpiece is achieved by successive iterations of the chemical and mechanical actions. The material removal rate (MRR) of CMP processes can be moderated using Preston's law, which dictates that the polishing rate is affected by the polishing pressure distribution, the polishing plate characteristics and the relative speed of the abrasives and the workpiece [11]. Usually, abrasives with submicron diameters and low hardness values are used in CMP for delicately removing raised surface materials and producing a damage-free and smooth surface. However, a major challenge of MP and CMP in metal finishing is the interference of rigid tools, which is absolutely indispensable and inhibits their application for finishing metal parts with significantly small and complex features.

In the past few decades, electropolishing (EP) has been widely used for polishing various metals, such as stainless steel [12], titanium [13], copper [14], aluminum [15] and tungsten [16], because of its high efficiency and stress-free procedure. During electropolishing, the workpiece to be polished acts as an anode and is oxidized into metal ions due to a loss of electrons. These ions dissolve into the electrolyte, resulting in

* Corresponding author.
E-mail address: dengh@sustech.edu.cn (H. Deng).

https://doi.org/10.1016/j.ijmachtools.2020.103517
Received 22 October 2019; Received in revised form 5 January 2020; Accepted 5 January 2020
Available online 10 January 2020
0890-6955/© 2020 Elsevier Ltd. All rights reserved.

the flattening of the surface. Although EP has been used for decades, its mechanism has not been fully understood [17]. From this perspective, Jacquet proposed a viscous film theory, which has been the most widely accepted theory [18]. A viscous liquid film comprised of dissolved oxidation products with a high viscosity and large electrical resistance is formed on the workpiece surface. The viscous liquid film that develops along the rough surface is not uniform, and the thickness at the depressed parts is greater than that at the raised parts. Therefore, the dissolution of the raised parts is relatively fast, resulting in macroscopic polishing of the rough surface. In addition, compared to other metal finishing techniques, EP has many advantages. The use of an aqueous electrolyte as the polishing media is suitable for parts with complex shapes [19], and the absence of mechanical interaction avoids SSDs and residual stresses on the surface [20]. In addition, as a potential driven material removal technique, electropolishing is simple and versatile in operation [21]. However, due to the vital role of the viscous layer in EP, the selection and optimization of the electrolyte for different metals becomes critically important [22].

In recent years, novel metal finishing techniques such as ion beam polishing (IBP), laser polishing (LP), magneto-rheological polishing (MRP) and multijet polishing (MJP), which are assisted by external energy sources have been proposed. IBP is a high precision and controlled process based on a physical sputtering phenomenon that is achieved by a well-focused ion beam operated in a vacuum chamber [23]. LP utilizes a laser with a certain energy density and wavelength to illuminate the surfaces of metal workpieces [24]. A thin layer of the surface melts, and the material of the peaks tends to flow into the valleys due to surface tension. After a laser beam treatment, the melted material solidifies, and the surface flattens. MRP utilizes the rapid relative movement of the workpiece and magnetic particles to remove the raised parts and produce a smooth surface [25]. MRP has good repeatability and is widely considered a deterministic polishing technique. In MJP, multiple fluid jets with respective pressure controls are used to polish complex surfaces with high machining accuracy and efficiency [26].

In the present study, an isotropic etching-based metal finishing process, i.e., isotropic etching polishing (IEP) with excellent surface finishing and high polishing efficiency, is proposed. The IEP etching anisotropy and the polishing characteristics of titanium have been investigated. Application results on stainless steel 304, aluminum alloy 6063 and pure nickel demonstrate that IEP is a promising, universal polishing approach for metal finishing. In addition, a theoretical IEP model has also been developed to comprehend the polishing process.

2. Principles of isotropic etching polishing

The surface smoothening mechanism of the proposed IEP process is illustrated in Fig. 1. The metal surface becomes passivated once the workpiece is immersed into an electrolyte with strong oxidizing properties. The workpiece is connected to the anode of a DC power supply because some weak sites of the passivation layer with small oxide thicknesses preferentially start breaking once the potential is high enough. At the breakdown sites, electrochemical etching takes place, and the metal surface dissolves. The etching anisotropy can be modulated by adjusting the etching temperature or the volume ratio of the electrolyte components. For most metals, electrolytes with a high volumetric ratio of dissolvent and a low temperature are preferred for realizing isotropic etching. At the beginning of the etching process, many initial breakdown sites are randomly distributed over the entire workpiece, where isotropic etching takes place at a later stage. Due to isotropic etching, the shape of the etching holes is hemispherical. As the etching duration increases, the diameters of the hemispherical etching holes become larger and start overlapping. Finally, the diameters of the hemispherical holes become large enough that the neighboring holes all merge together. As a result, the entire rough surface is completely replaced by the smooth inner surface of the merged hemispherical etching holes. Theoretically, the larger the holes grow, the smoother the etched surface will be. In addition, the passivation layer localizes the isotropic etching and falls off once the metal underneath is completely dissolved.

After polishing, once the DC power is turned off, a passivation layer is immediately formed on the surface due to the oxidizing ability of the electrolyte. It is well known that such passivation film is helpful in protecting the metal substrate from corrosion without influencing the surface roughness.

It is noteworthy that IEP, compared to conventional EP, has a different smoothening mechanism, regardless of the electrochemical nature of both processes. Metal surface polishing by IEP is based on the merging of randomly distributed isotropic etching sites, whereas the diffusion layer plays a key role in EP [27]. As the diffusion layer that is formed in EP will generally increase the resistance in a polishing loop, the energy consumption in IEP is considered more efficient. In terms of the polishing mechanism, the principle of surface variation between EP and IEP is different. The surface variation is a process of gradual leveling for EP; in contrast, due to the growth of etching holes in IEP, the surface roughness increases first and then consistently decreases. Therefore, the change in surface roughness is an important feature for distinguishing between EP and IEP. Another important difference are the solution requirements. The solution for EP with different metal materials is

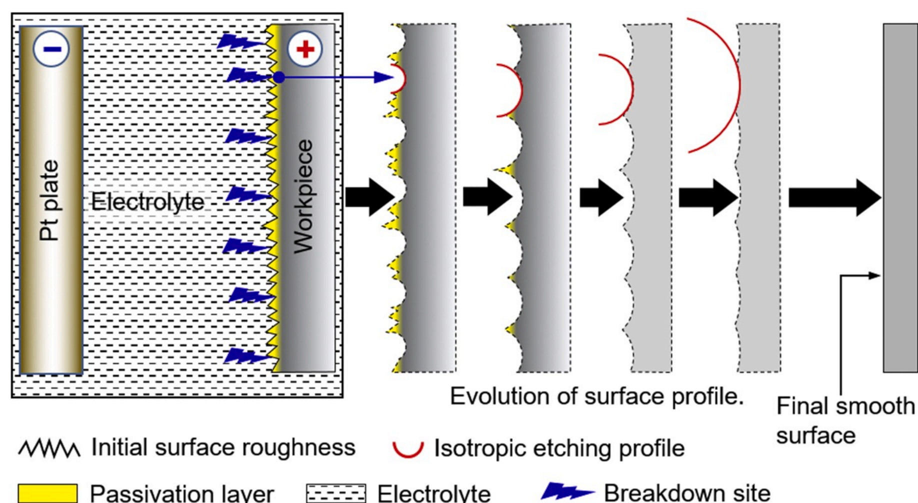

Fig. 1. Schematic of the surface smoothening mechanism of IEP.

determined by the different solubility properties of metals in different solutions. However, IEP is a more universal method that allows polishing of different metals while using the same polishing solution. In summary, EP and IEP are two different polishing methods in terms of the polishing mechanism, energy efficiency, variation principle of surface morphology and selection of electrolyte.

To theoretically show the feasibility of IEP, the etching process was modeled. Initially, a fast Fourier transform (FFT) analysis was used to simulate the initial rough surface [28]. A two-dimensional matrix was randomly generated, and the matrix size was considered as a pixel number of a surface measurement. Then, Fourier transformation was performed on the random matrix, and the result was multiplied by an autocorrelation function, which described the degree of correlation between data at different locations. Finally, an inverse Fourier transformation was performed on the product, and the raised heights of the original simulated rough surface were obtained.

The expression of the autocorrelation function in an exponential form is as follows [29]:

$$H = \exp\left(-2.3 \times \left(i^2 + j^2\right)^{0.5} \Big/ \beta\right) \ \mathrm{i, j} = 1, 2, \ldots, \mathrm{N} \tag{1}$$

where β represents the length of autocorrelation.

The expression of the original surface is as follows:

$$f_O = z - \left\{\mathscr{F}^{-1}[H \cdot \mathscr{F}(N)]\right\} \tag{2}$$

where z and H represent the height and autocorrelation functions, respectively.

According to Fig. 1, the etching holes were hemispherical and randomly distributed, so the expression of the etching hole surface can be given as:

$$f_H = \sum_1^n \left[R_k{}^2 - (x - x_{r_k})^2 - (y - y_{r_k})^2 - (z - z_{r_k})^2\right] \tag{3}$$

$$f_O(x_{r_k},\ y_{r_k},\ z_{r_k}) = 0 \tag{4}$$

where x_{r_k}, y_{r_k} and z_{r_k} refer to the random spatial position of the etching hole; furthermore, the coordinates of each etching point should be located on the random surface, as described by Equation (4). R_k refers to the radius of the hemispherical hole. By combining Equations (2) and (3), we obtain a surface height expression that represents a random rough surface with hemispherical polished holes as follows:

$$\mathrm{F} = \mathrm{Max}\{f_O,\ f_H\} \tag{5}$$

A simulation of the IEP process has been conducted to investigate the evolution of surface morphology with isotropic etching. Fig. 2 shows the variation progress of surface topography when there are 10 hemispherical etching holes gradually growing from an R_k of 0.2 μm to an R_k of 50 μm. The randomly distributed hemispherical holes that appear in the early etching stage are shown in Fig. 2(b). As the hemispherical holes gradually grow, the neighboring holes start overlapping with each other. After a certain etching duration, the original rough surface is completely removed and replaced by the inner surface of the hemispherical holes. At the beginning of operation, the workpiece becomes rougher, as shown in Fig. 2(a–c). However, with the growing holes on the surface, the workpiece becomes smoother, as shown in Fig. 2(d–f).

The surface average roughness *Sa* at different etching evolution stages can be calculated by the equation below:

$$Sa = \frac{\sum_1^n |Z_k - \overline{Z}|}{n} \tag{6}$$

According to the surface smoothening model of IEP, the surface Sa roughness can be simulated as shown in Fig. 3. It is necessary to note that

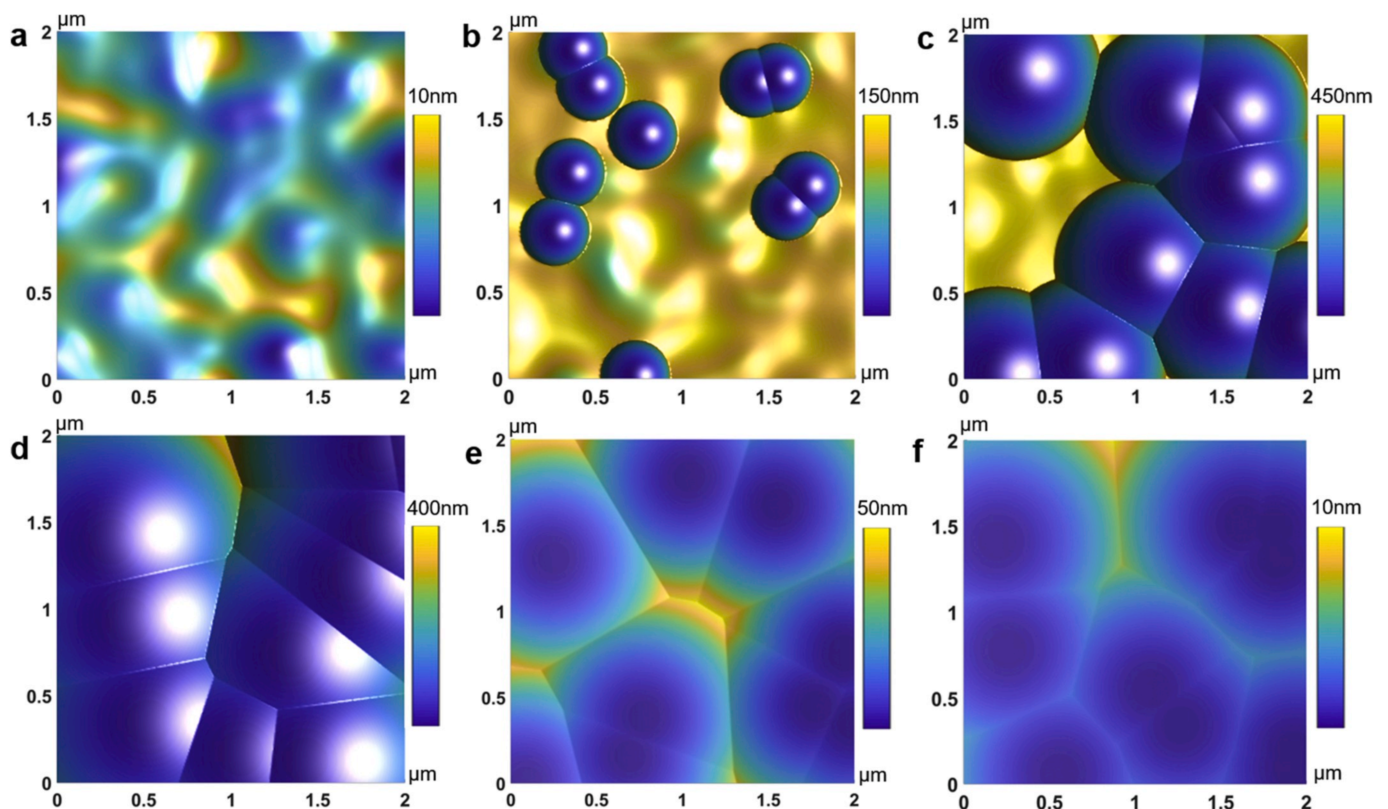

Fig. 2. Simulated surface morphologies with isotropic etching: (a) the original surface (32.7 nm in Sa), (b) R is 0.2 μm (58.8 nm in Sa), (c) R is 0.5 μm (162.4 nm in Sa), (d) R is 1 μm (47.8 nm in Sa), (e) R is 10 μm (4.1 nm in Sa) and (f) R is 50 μm (1.3 nm in Sa).

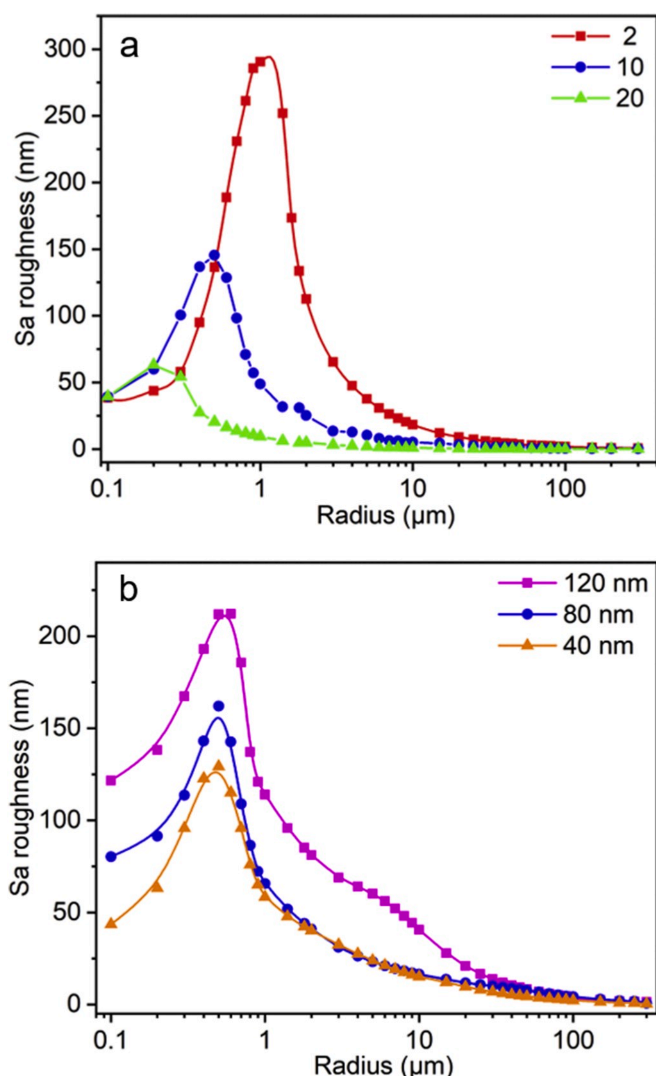

Fig. 3. Predicted Sa roughness with different radii of isotropic etching holes: (a) radii of 2, 10, and 20 for the etching holes on the 2x2 μm^2 metal surface; and (b) when the initial Sa roughness is 40 nm, 80 nm, and 120 nm.

the roughness values shown in Fig. 3 are predicted by the model and have not been experimentally verified. These curves indicate how the surface can be smoothed as well as the key factors affecting this smoothening process. Fig. 3(a) is plotted under the condition that there are 2, 10 and 20 isotropic etching sites within an area of $2 \times 2\ \mu m^2$, and the initial Sa is 36 nm. As shown in Fig. 3(a), all the roughness curves follow the same trend, and the Sa roughness eventually approaches zero. It is found that a relatively high density of etching holes on the surface can significantly improve the polishing efficiency of IEP. Fig. 3(b) is plotted under the condition that there are 10 isotropic etching sites within an area of $2 \times 2\ \mu m^2$, and the three curves have different initial Sa values of 40 nm, 80 nm, and 120 nm. As shown in Fig. 3(b), all the roughness curves follow the same trend. For a high Sa roughness value, the decreasing rate of its curve with respect to the radii of the etching holes is higher than the other curves with low initial Sa roughness values. The results indicate that the Sa roughness values of a relatively smooth surface approach zero sooner in IEP.

Based on the results of the surface morphology simulation and the roughness prediction, the theoretical feasibility of IEP for surface smoothening has been confirmed. With the random growth and continuous merging of isotropic etching holes, a smooth surface can eventually be obtained under optimized conditions. The density of the etching hole and the initial surface roughness do not affect the final polishing performance, and more etching holes formed on the surface will lead to a faster surface polishing speed.

3. Experimental approach

The etching anisotropy of TA2 (pure titanium: Fe $\leq$ 0.30, C $\leq$ 0.08, N $\leq$ 0.03, H $\leq$ 0.015, O $\leq$ 0.25, Ti $\geq$ 99.325) was systematically studied, including the conditions of isotropic etching, the form and surface roughness of the isotropic etching holes, the proof of localized breakdown of the passivation layer and the density of the isotropic etching sites. Additionally, the IEP of TA2 was experimentally studied, including the evolution of surface morphology, the change in surface roughness and the MRRs with different etching currents. To investigate the universality of IEP, a variety of metals, including stainless steel 304, aluminum alloy 6063 and pure nickel substrates, were also tested.

Commercially available substrates with a diameter of 15 mm and thickness of 3 mm were used in this study. Only one side of the substrate was polished. Before IEP, the substrates were lapped by SiC sandpapers (#500) to remove the rough slicing marks introduced by wire cutting. Then, to remove contaminants, the substrates were ultrasonically cleaned in deionized water and ethyl alcohol for 5 min. A glass beaker containing electrolyte was used as a reaction cell. A platinum mesh ($2 \times 2\ cm^2$) was connected to the negative terminal, while the workpiece was connected to the positive terminal of a DC power supply (Keysight E3649A dual output). The distance between the cathode and anode was kept constant at 60 mm. The current and voltage recorded during the experiment were output to a connected computer.

The IEP electrolyte has two functions: passivation of the metal surface and electrical dissolution of the metal surface at the breakdown sites. Thus, analytical grade H_2SO_4 (97%) and CH_3OH (99.5%) were used as the electrolyte. H_2SO_4 plays the role of passivation and etching, while CH_3OH acts as an efficient destabilizing agent of the surface oxide films [30]. At the surface of the anode, an oxidation reaction occurs and then the oxide is dissolved into the electrolyte. Meanwhile, a reduction reaction occurs around the cathode. The reactions occurring on the cathode and anode are listed as follows:

$$\text{Cathode: } 2nH_2SO_4 + 2ne^- \rightarrow nSO_2 + nSO_4^{2-} + 2nH_2O \quad (7)$$

$$\text{Anode: } 2M(s) \rightarrow 2M^{n+} + 2ne^- \quad (8)$$

After polishing, the substrates were ultrasonically cleaned in deionized water before characterization. All experiments were carried out at room temperature. The surface morphology was examined by scanning electron microscopy (SEM, ZEISS Merlin). The surface roughness was measured by atomic force microscopy (AFM, Bruker Edge). The surface profile was measured by a laser scanning confocal microscope (LSCM, Keyence VK-X1000). The material removal rate was evaluated by conversion from the loss of weight.

4. Etching anisotropy of titanium

According to the principle of IEP, one prerequisite of surface smoothening is that the etching process must be isotropic. The anisotropy for the electrochemical etching of aluminum has been reported [31]. According to the etching mechanism, the anisotropy is dependent on various factors, such as the temperature, potential and electrolyte concentration. In this study, the electrolyte concentration was modulated to control the etching anisotropy. TA2 substrates were etched at a constant current of 0.02 A for 1 min in two electrolytes with 1% and 10% volume ratios of H_2SO_4 to CH_3OH.

At room temperature, the crystal structure of TA2 is hexagonal-close-packed (hcp) with lattice parameters of a = 0.2950 nm and c = 0.4683 nm [32], as shown in Fig. 4(a). Fig. 4(b–d) shows the morphology of the TA2 pits after being etched in electrolyte with a 1% volume ratio of H_2SO_4 to CH_3OH. Anisotropic etching pits with different shapes were

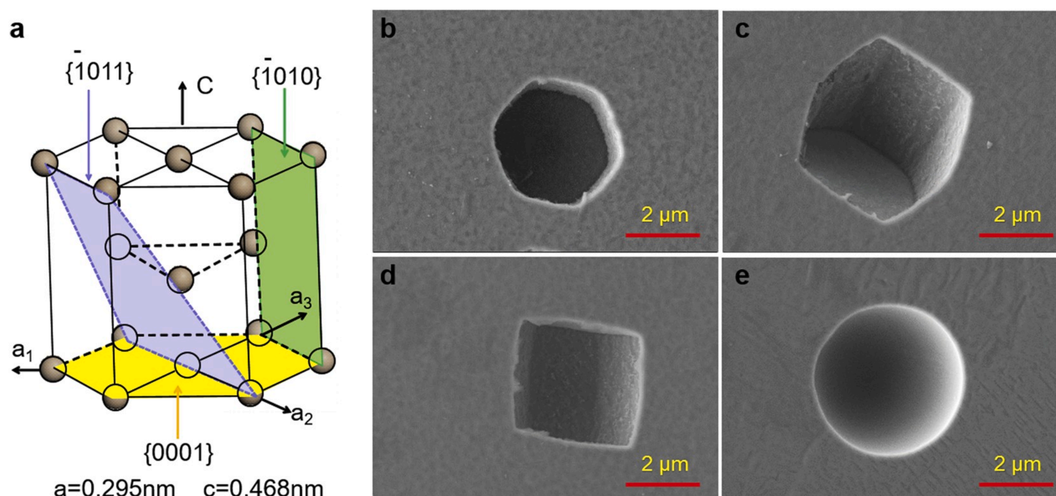

Fig. 4. Crystal structure of TA2 (a), typical surface morphology after etching in electrolytes with a 1:100 vol ratio of H_2SO_4 to CH_3OH (b), (c), (d); and in electrolytes with a 10:100 vol ratio of H_2SO_4 to CH_3OH (e).

formed on the surface. Similar results were reported in the etching of a Ti–V alloy and a ZrTiAlV alloy [33,34], and the formation of anisotropic etching pits were explained by different crystalline faces having different etching rates. Because of a disparate supply of H_2SO_4, the different atom densities on {-1010} and {0001} led to different etching rates and the formation of anisotropic etching pits. The shape of the etching pits was similar to that of the hcp structure placed at different angles. As a polycrystalline material, the titanium grains in TA2 had different orientations. In Fig. 4(b), (c), and (d), the angles between the workpiece surface and the {0001} crystalline face are approximately 0°, 45° and 90°, respectively. Because of the orientation dependence of the etching pit morphology, it was difficult to obtain a smooth TA2 surface with isotropic etching, regardless of the high pit density on the surface.

However, with a 10% volume ratio of H_2SO_4 to CH_3OH, the etching pits developed in a round shape, as shown in Fig. 4(e), and with a sufficient supply of H_2SO_4, the variance in the etching rates of different crystalline faces became insignificant, resulting in an isotropic etching process.

As shown in Fig. 4(e), the isotropic etching hole was hemispherical in shape with an extremely smooth inner surface. Normally, the IEP etching process must be isotropic, and the final surface roughness was strongly determined by the roughness of the inner surface of the holes. Therefore, the shape and inner surface roughness of the etching holes were determined, and the results are shown in Fig. 5. To increase the number of etching sites for the convenience of the profile and inner surface investigation, a high current of 0.1 A was applied for 1 min. As seen from Fig. 5(a), the etching holes were randomly distributed on the

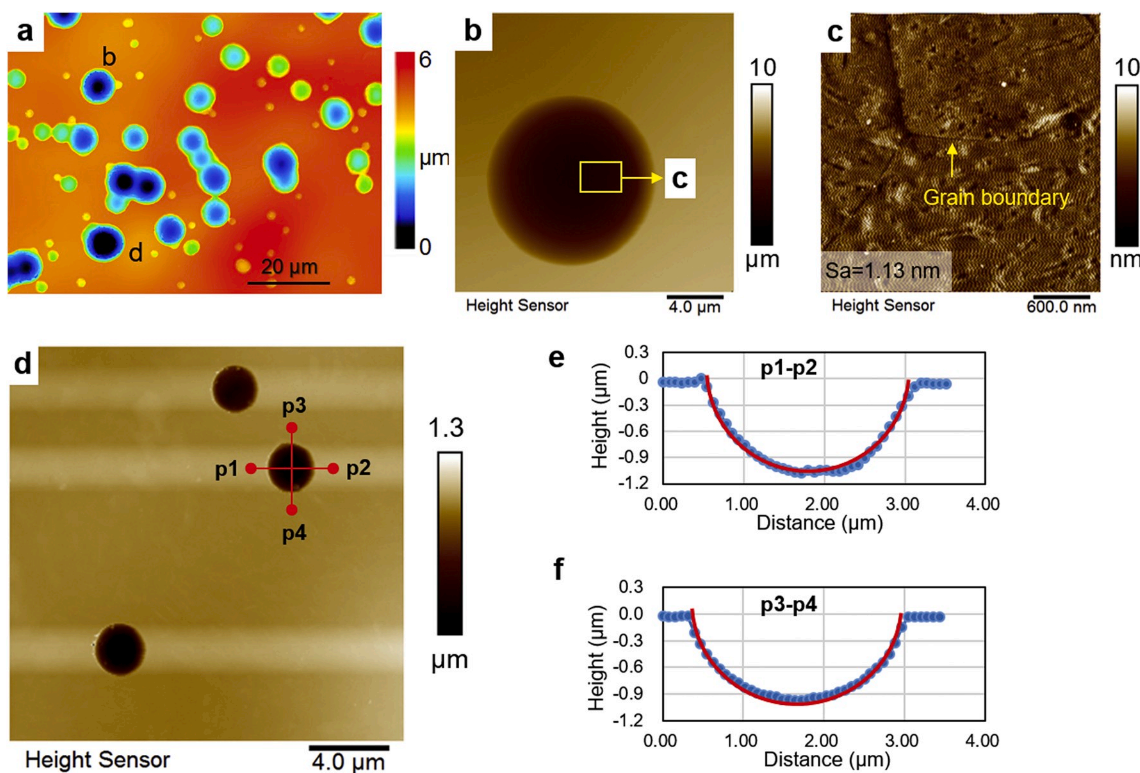

Fig. 5. Morphology of isotropic etching holes formed on TA2. (a) Overall morphology observed by LSCM, (b, c) close-up view of a large etching hole and its inner surface roughness measured by AFM and (d, e, f) close-up view of some small etching holes and cross-sectional profiles measured by AFM.

substrate surface. The radii of the etching holes varied from a few microns to approximately 10 μm, while some of them were interconnected with adjacent holes. The variation in the radii of these etching holes was caused by the inhomogeneity of the passivation film. As the film preferentially broke down in relatively weak areas, the etching durations for different etching holes were not exactly the same, resulting in varying radii of the etching holes. However, according to the mechanism of IEP, only holes with large radii contributed to the surface smoothening process as the small holes were gradually annihilated. Thus, it was considered that the variation in the radii of the holes would not affect the polishing performance of IEP.

From the top view, these etching holes appeared to be hemispherical. Some of these etching holes were profiled by AFM to investigate their inner roughness. In Fig. 5(b), a large etching hole with a diameter of more than 10 μm is shown, while the morphology of the inner surface is shown in Fig. 5(c). An insignificant *Sa* roughness value (1.13 nm) showed that the inner surface of the etching hole was smooth. However, the presence of slight undulations was thought to be caused by generic defects in TA2. Additionally, the grain boundaries were also observed, as marked in Fig. 5(c). Some small etching holes with a diameter of approximately 3 μm were also observed, as shown in Fig. 5(d). Fig. 5(e) and (f) show the semicircular horizontal and vertical profiles of an etching hole from Fig. 5(d).

As shown in Fig. 5(a), the isotropic etching holes were randomly distributed on the etched surface, which was attributed to the random breakdown of the passivation layer. However, owing to the small thickness of the passivation layer [35], it was difficult to experimentally demonstrate the breakdown phenomenon. Thus, in this study, a pre-oxidized surface was used to investigate the breakdown and etching process. A TA2 substrate was anodically oxidized in 1 wt% NaOH solution for 10 s with an applied electric potential of 15 V. According to ellipsometry measurements, an oxide layer with a thickness of 35.4 nm was formed as the result of anodization. Then, this surface was further processed by electrochemical etching in a 10% volume ratio of H_2SO_4 to CH_3OH at a 1 A current for 1 min. As shown in Fig. 6(a), there existed an obvious breakdown site in the center of the etching hole. The oxidation film remained intact on the surface, whereas TA2 beneath the layer was gradually dissolved. The LSCM picture of the etching hole is shown in Fig. 6(b). In the middle of the etching hole, a small breakdown site was also observed. The profile of the etching hole is illustrated in Fig. 6(c). Due to the existence of the passivation layer, no semicircular structure appeared in the profile. However, a deep hole appeared in the middle of the profile, which was the breakdown site. These results proved that the formation of isotropic etching holes is due to the protective effect of the oxidation film. Initially, breakdown occurred at the weak sites of the oxide film, and then the metal underneath dissolved, while etching occurred around this breakdown point and formed a hemispherical hole in the end. For normal polishing cases, the passivation layer was too thin to sustain the etching holes and was removed by dropping down, water rinsing or ultrasonic vibration.

It was demonstrated that TA2 could be isotropically etched with a smooth inner surface. As the IEP of metals was based on merging isotropic etching holes, the hole density strongly affected the surface roughness and polishing efficiency. Therefore, a series of experiments were carried out to study the influence of the current on the density of the etching holes. These experiments were performed at currents of 0.01, 0.05, 0.1, 0.2, 0.5 and 0.8 A for a constant duration of 5 s in an electrolyte with a 10% volume ratio of H_2SO_4.

The morphologies of the etched surfaces with different currents are shown in Fig. 7. Though many lapping marks developed on the initial surface, the etching holes were randomly formed without preference to the lapping mark locations. It was found that the hole density increased with an increase in the current. When the current was 0.01, 0.05 and 0.1 A, only a few etching holes were formed owing to the low etching potential, as shown in Fig. 7(a, b, c). As shown in Fig. 7(d and e), when the current was further increased to 0.2 A and 0.5 A, on one side, the hole

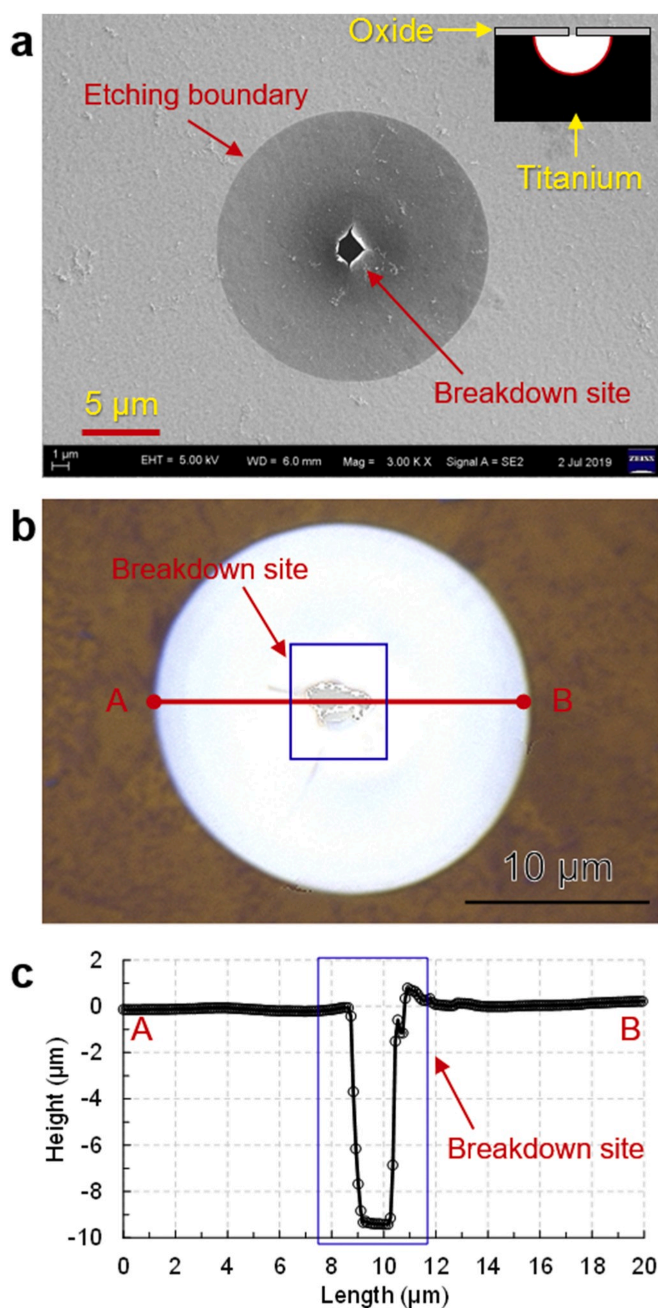

Fig. 6. Images of the localized breakdown of the oxidized TA2 surface during electrochemical etching. (a) SEM image, (b) LSCM image and (c) cross-sectional profile of the etching hole measured by LSCM.

density increased remarkably, while on the other side, the size of the holes was reduced, compared with the holes produced at lower currents. However, at 0.8 A the etching holes became large, and some smooth areas were formed, which was possibly the result of the holes merging, as shown in Fig. 7(f).

From the previous discussion, it could be inferred that the current affects both the density and the growth rate of the holes. When the current was lower than 0.1 A, although a few sites were broken down, the size of the holes size were large, which was attributed to their large electric flux. In contrast, when the current was higher than 0.2 A but lower than 0.8 A, more sites were broken down due to the large etching potential; however, the hole size was small owing to their small shared electric flux. When the current was higher than 0.8 A, a large density and a high growth efficiency of the holes could be simultaneously realized.

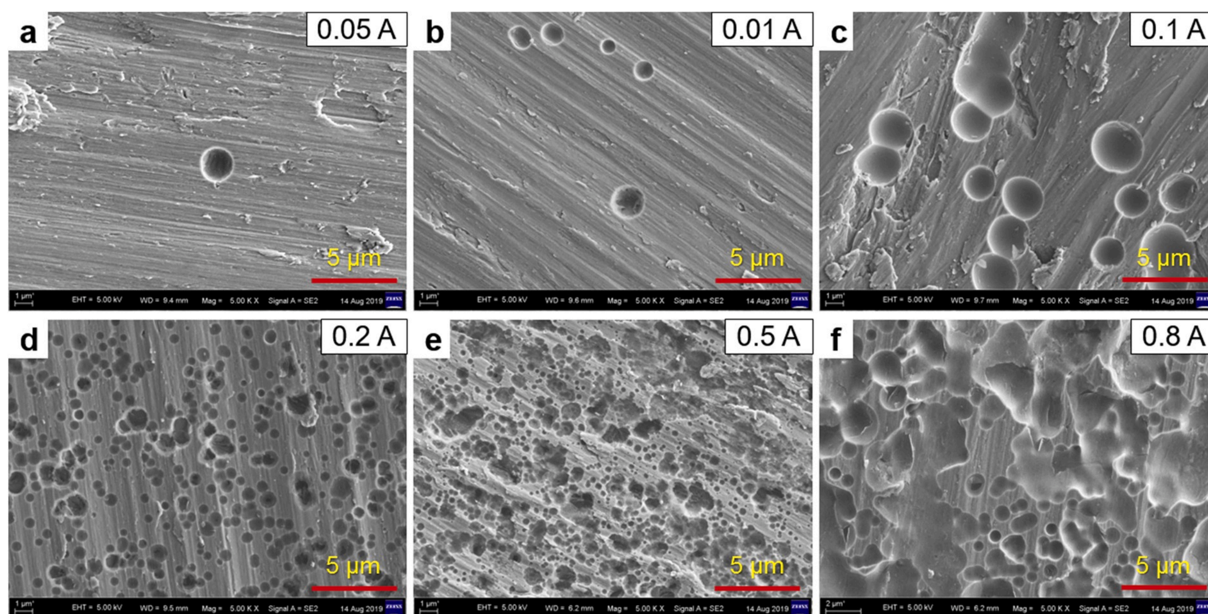

Fig. 7. Morphologies of the TA2 surfaces etched at different currents: (a) 0.01 A, (b) 0.05 A, (c) 0.1 A, (d) 0.2 A, (e) 0.5 A and (f) 0.8 A.

Thus, to obtain a smooth surface with a high efficiency, an applied current higher than 0.8 A was preferred. According to the section describing the IEP model, the metal surface will eventually be polished by increasing the etching duration even if the current is relatively low. However, polishing efficiency is important for the practical application of IEP. According to Fig. 3, the efficiency of IEP is generally affected by two factors: hole density and hole growth rate. As shown in Fig. 7, the current played an important role in determining both the hole density

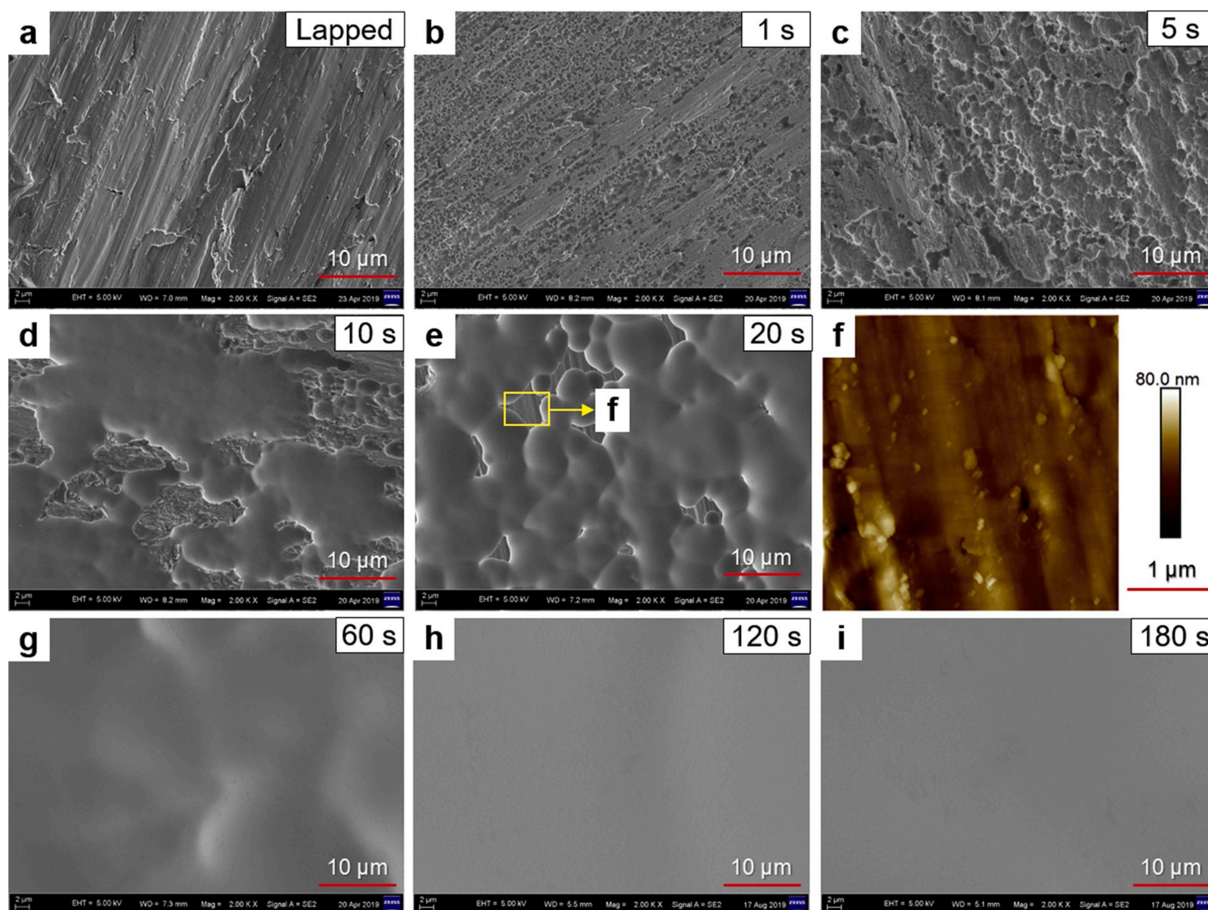

Fig. 8. Surface morphology evolution of TA2 during IEP observed by SEM and AFM. (a) Original surface, (b) 1 s, (c) 5 s, (d) 10 s, (e) 20 s, (f) AFM image of the raised part from figure (e), (g) 60 s, (h) 120 s and (i) 180 s.

and hole growth rate. Thus, the current was an important parameter for realizing highly efficient metal finishing.

5. Isotropic etching polishing of titanium

Based on the etching anisotropy of titanium, IEP of TA2 was conducted under optimized conditions for investigating the evolution of the surface morphology, the polished surface roughness and the polishing efficiency. First, TA2 was etched at a constant current of 1 A for different durations of 1, 5, 10, 20, 60, 120 and 180 s to study the surface morphology evolution. The changes in surface topography shown in Fig. 8 were found to be consistent with the simulation results shown in Fig. 2. As shown in Fig. 8 (a), there were many marks on the original substrate surface introduced by lapping. After etching for 1 s, many small isotropic etching holes were randomly formed on the surface, which started intersecting, and the nonetched residual area was reduced after etching for 5 s. After etching for 10 s, the residual area was further reduced, and some smooth basin structures were formed because of the etching holes combining further. After etching for 20 s, only a few residual “island”-like areas were left on the surface. The morphologies of these “island”-like areas were observed using AFM and some lapping marks could still be clearly observed; this indicated incomplete material removal at these sites, as shown in Fig. 8(f). After etching for 60 s, the residual areas were completely removed, and a smooth surface was obtained; however, minute signs of waviness could still be observed. Finally, after etching for 120 s and 180 s, the surface became significantly flat, and there were no signs of waviness, as shown in Fig. 8(h) and (i). To summarize the results shown in Fig. 8, the surface smoothening process was ideally consistent with the proposed isotropic etching-based polishing mechanism.

The AFM images and the profile of the original surface are shown in Fig. 9(a) and (c). Lapping marks were observed on the original surface, which was consistent with the SEM observation shown in Fig. 8(a). The AFM images and profile of the IEP processed surface at 1 A for 3 min are shown in Fig. 9(b) and (d), and they show that the surface has been efficiently smoothened and that the *Sa* roughness value was reduced from 64.1 to 1.23 nm. The optical photos before and after etching are shown in Fig. 9(e) and (f), and they demonstrate that a mirror-like surface is obtained by IEP.

Fig. 9(g) shows the *Sa* roughness of the TA2 substrate etched for different durations. Compared with the original lapped surface, the *Sa* roughness increased first and then decreased with increasing etching duration. The increasing *Sa* roughness was considered a consequence of the generation of numerous isotropic etching holes, while the decrease in the *Sa* roughness was attributed to the merging of the etching holes. The drastic drop in *Sa* roughness belongs to the critical moment when the substrate surface was completely replaced by etching holes. The experimental data shown in Fig. 9(g) coincides well with the simulation results shown in Fig. 3, which proves the effectiveness of the proposed IEP model. Fig. 9 (h) shows the MRRs of IEP at different currents. The removal efficiency gradually increased with increasing current. When the current was 3 A, the MRR reached 16 μm/min, proving that IEP was a highly efficient polishing approach for TA2.

For further investigation of the surface finishing capability of IEP, a two-phase titanium alloy TC4 was also tested by IEP. Finishing of multiphase materials is difficult owing to the different mechanical or chemical properties of different phases [36–38]. Fig. 10(a) shows the XRD pattern of the TC4 substrate. The major α-Ti phase and minor β-Ti phase were both detected. It was considered that α-Ti and β-Ti might have different etching rates during electrochemical etching. However, it was found that isotropic etching of TC4 could be realized with a 10% volume ratio of H_2SO_4 to CH_3OH, a current of 0.1 A and a duration of 2 min, as shown in Fig. 10(b). Fig. 10(c) and (d) show the AFM images and profiles of the original lapped surface and the IEP processed surface. The *Sa* roughness was reduced from 24.2 nm to 2.04 nm, demonstrating that IEP was also applicable to TC4. According to the profile in Fig. 10(d), α-Ti had a higher etching rate than β-Ti, which resulted in the formation of convex β-Ti structures.

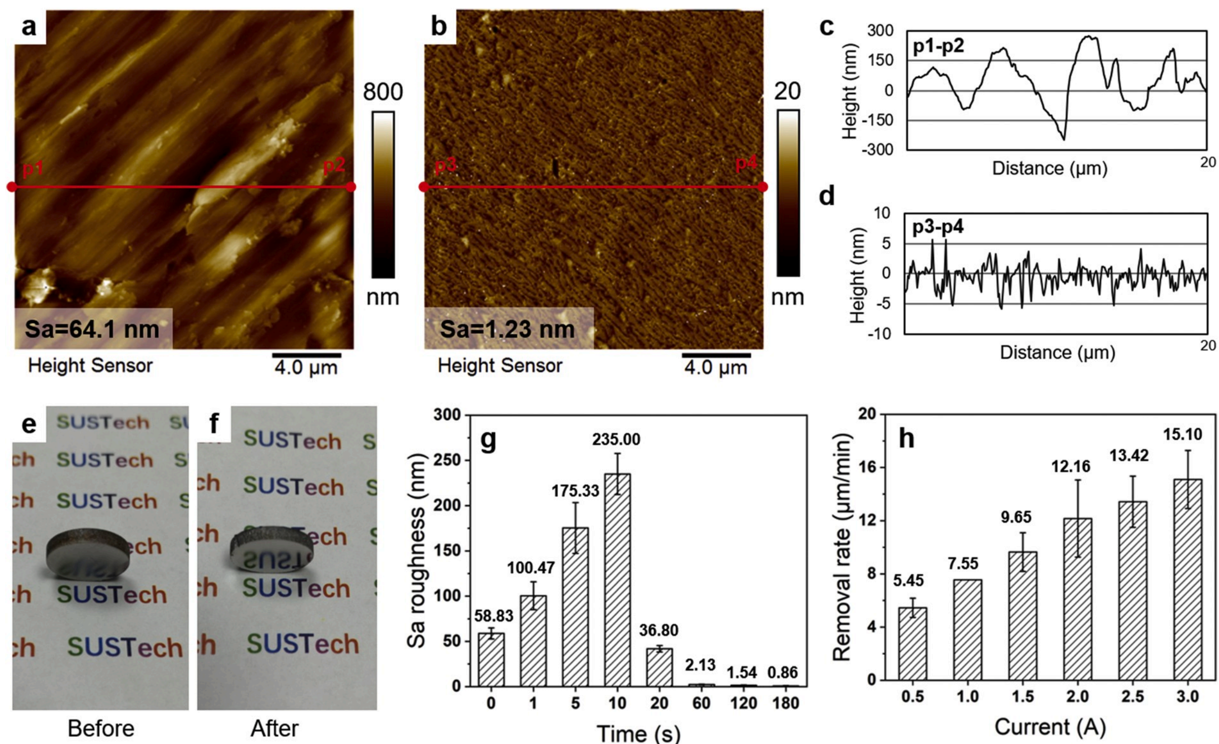

Fig. 9. AFM images, surface profiles and optical pictures of the original surface (a, c, e) and etched surface (b, d, f) at a current of 1 A for 3 min; (g) surface roughness values versus time, and (h) removal rates versus current.

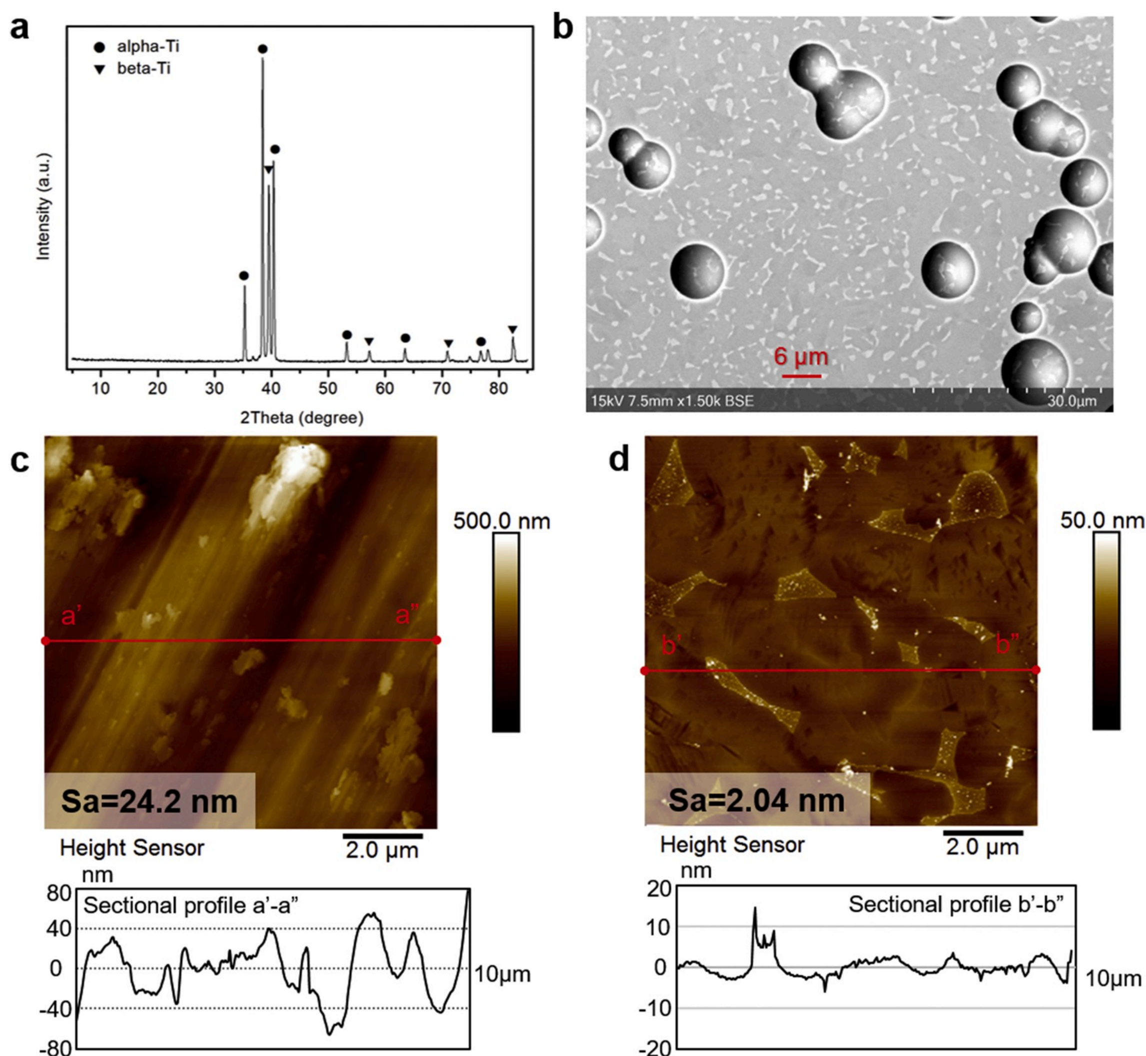

Fig. 10. (a) XRD pattern of the TC4 substrates, (b) isotropic etching holes formed on TC4 (0.1 A and 2 min), (c) AFM image and surface profile of the original lapped surface and (d) AFM image and surface profile of the IEP processed surface.

6. Isotropic etching polishing of metals

According to the surface smoothening mechanism of IEP, it can be considered a universal finishing approach for different metals, as most metals can be passivated and electrochemically dissolved [39–41]. To verify the universality of IEP, it has been applied to stainless steel 304, aluminum alloy 6063, and pure nickel, and the results are shown in Fig. 11.

It is noteworthy that the polishing parameters of TA2 cannot be directly applied on stainless steel 304, aluminum alloy 6063 and pure nickel because of their different properties. Therefore, exploratory experiments were carried out to identify the optimized polishing parameters, such as the volume ratio (H_2SO_4:CH_3OH), etching current and polishing duration, for different metal materials. The volume ratio was tuned to realize an isotropic etching process. The etching current was optimized to guarantee the density of etched holes and their growth rate. Finally, the required polishing time was carefully investigated to improve the surface finish through a number of experiments.

The 304 stainless steel was polished by an electrolyte with a 20% volume ratio of H_2SO_4 to CH_3OH at a current of 0.5 A. The random distribution of the etching holes on the stainless steel surface that was etched for 60 s, and the additional details of an isotropic hole are shown in the insert of Fig. 11(a1). Fig. 11(a2) shows the lapped surface, while Fig. 11 (a3) shows a 2 min IEP process that efficiently smooths the surface and reduce the *Sa* roughness from 14.6 nm to 0.72 nm.

The aluminum alloy 6063 was etched in an electrolyte with a 30% volume ratio of H_2SO_4 to CH_3OH at a current of 3 A. When the etching duration was 2 s, isotropic etching holes were randomly distributed on the surface, as shown in Fig. 11(b1). However, the sizes of the etching holes were smaller compared to those of the stainless steel sample, which was attributed to the high current and short duration. Smooth basin-like structures were formed on the surface, which was consistent with the IEP finishing process of titanium. The insert shows the details of an isotropic etching hole on an aluminum alloy. Fig. 11(b2) and (b3) shows the lapped and IEP processed (1 min) surfaces, respectively. Although the original surface had an initial *Sa* roughness of 53.5 nm, it was reduced to 2.90 nm after IEP for 1 min. These results demonstrate that the polishing of aluminum alloy 6063 by IEP was also feasible. In addition, the presence of some protrusions on the polished surface was due to certain additives on the substrate.

The nickel was etched in the electrolyte with a 10% volume ratio of H_2SO_4 to CH_3OH at a current of 0.5 A. The surface morphology evolution during etching was similar to the previously mentioned metals. As shown in Fig. 11(c1), when the etching duration was 10 s, hemispherical etching holes were distributed on the whole surface. It was found that these etching holes were either very large "several μm" or very small "several tens of nm" in diameter. After IEP for 2 min, the *Sa* roughness was reduced from 75.9 nm to 0.89 nm, indicating a remarkably smooth

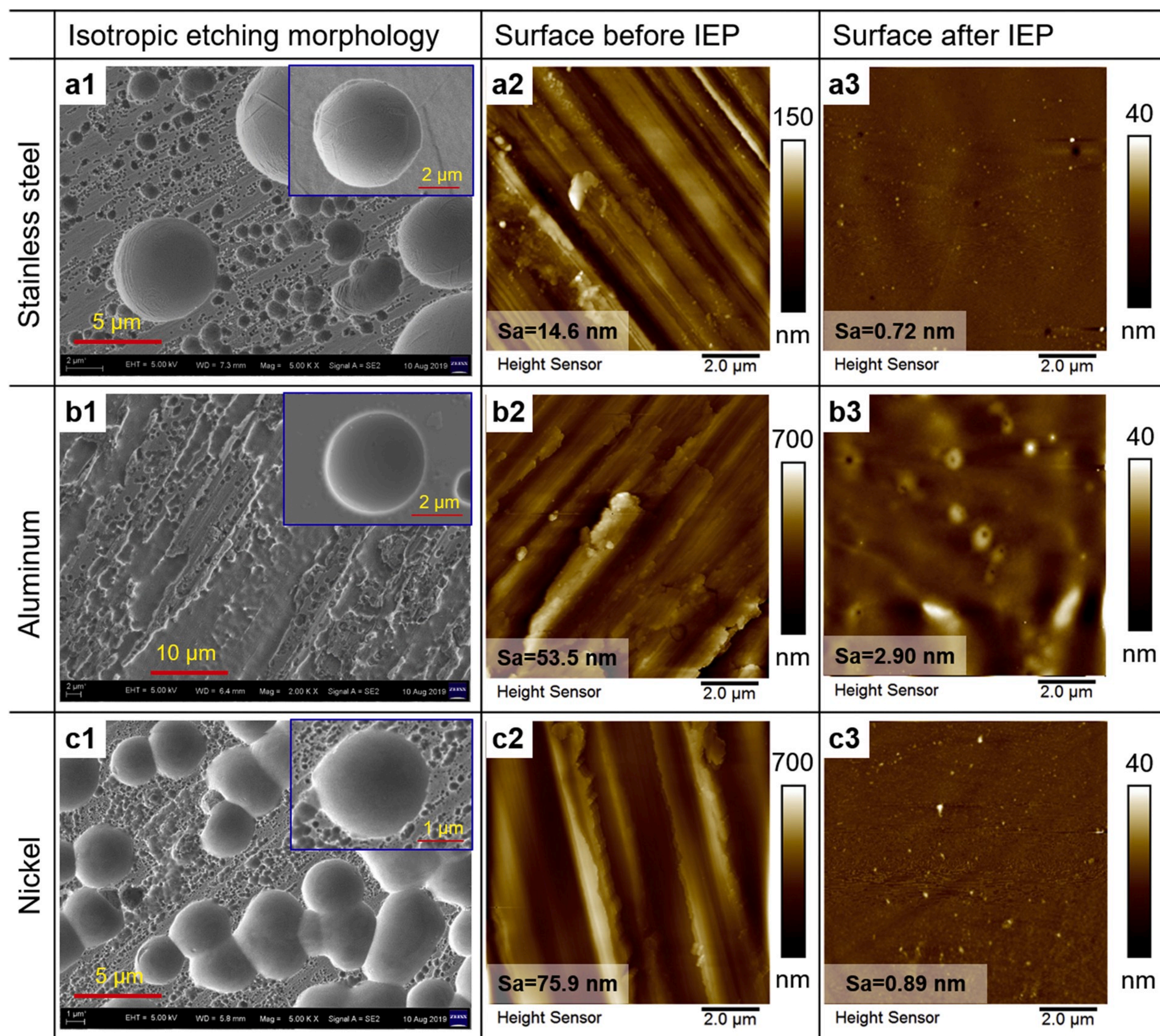

Fig. 11. Surface morphologies and roughnesses of different metals: (a1, a2, a3) 304 stainless steel, (b1, b2, b3) aluminum alloy 6063 and (c1, c2, c3) pure nickel.

surface, as shown in Fig. 11(c2) and (c3), which showed that IEP was also an effective technique for nickel.

Based on the application results of IEP, it is concluded that IEP is a promising universal metal polishing approach. Although some metal polishing techniques, such as EP [17], IBP [23], LP [24], MRP [25], and MJP [26], already exist, IEP is superior from the perspective of its universal polishing mechanism and versatile polishing setup, which produces an undamaged polished surface.

7. Conclusions

In this paper, a new universal metal finishing method based on isotropic electrochemical etching was proposed. The polishing process of IEP includes the formation, growth and merging of isotropic etched holes on the metal surface, which has been quantified by modeling and verified by being applied to different metals. The following conclusions can be drawn from this study:

- Etching of TA2 is anisotropic, when the volume ratio of electrolytes was set to 1:100 (H_2SO_4:CH_3OH). Etching will become isotropic when the volume ratio of electrolytes is increased to 10:100, and the inner surfaces of the isotropic etching holes are smooth with an Sa roughness of 1.13 nm.
- The etching holes are generated by a breakdown of the passivation layer. The etching current affects both the density and the growth rate of holes. For TA2, a high current that is larger than 0.8 A is preferred.
- IEP is effective and efficient for surface finishing of titanium. For TA2, the *Sa* roughness can be reduced from 64.1 nm to 1.23 nm, while for TC4, the *Sa* roughness can be reduced from 24.2 nm to 2.04 nm. The MRR is positively related to the current, and a maximum MRR of 15 μm/min can be achieved with a current of 3 A.
- IEP is also effective for surface finishing of other metals, such as stainless steel 304, aluminum alloy 6063 and pure nickel. Therefore, IEP can be considered a universal approach for metal finishing.

CRediT authorship contribution statement

Rong Yi: Data curation, Formal analysis, Writing - original draft. **Yi Zhang:** Validation. **Xinquan Zhang:** Methodology, Writing - review & editing. **Fengzhou Fang:** Conceptualization, Writing - review & editing. **Hui Deng:** Conceptualization, Supervision, Writing - review & editing.

Acknowledgements

This work was financially supported by the research fund for International Cooperation (GJHZ20180928155412525 and

GJHZ20180411143558312) from the Science and Technology Innovation Committee of Shenzhen Municipality, China. The authors also would like to thank the Shenzhen High-level Innovation and Entrepreneurship Fund (No. KQTD20170810110250357) for their financial support.

References

[1] K.M. Kawanaka T, Mirror-like finishing by electrolyte jet machining, CIRP Ann. - Manuf. Technol. 64 (2015) 237–240.
[2] K. Nestler, F. Böttger-Hiller, W. Adamitzki, G. Glowa, H. Zeidler, A. Schubert, Plasma electrolytic polishing – an overview of applied technologies and current challenges to extend the polishable material range, Procedia CIRP 42 (2016) 503–507.
[3] F. Hashimoto, H. Yamaguchi, P. Krajnik, K. Wegener, R. Chaudhari, H.-W. Hoffmeister, F. Kuster, Abrasive fine-finishing technology, CIRP Annal. 65 (2016) 597–620.
[4] J. Zhang, J. Hu, H. Wang, A.S. Kumar, A. Chaudhari, A novel magnetically driven polishing technique for internal surface finishing, Precis. Eng. 54 (2018) 222–232.
[5] Y. Takaya, K. Hida, T. Miyoshi, T. Hayashi, A novel surface finishing technique for microparts using an optically controlled microparticle tool, CIRP Ann. - Manuf. Technol. 55 (2006) 613–616.
[6] W.B. Kim, S.J. Park, B.K. Min, S.J. Lee, Surface finishing technique for small parts using dielectrophoretic effects of abrasive particles, J. Mater. Process. Technol. 147 (2004) 377–384.
[7] Qingliang Zhao, Zhiyuan Sun, Bing Guo, Material removal mechanism in ultrasonic vibration assisted polishing of micro cylindrical surface on SiC, Int. J. Mach. Tool Manuf. 103 (2016) 28–39.
[8] Ange Lu, Jin Tan, Qifeng Liu, Zongfu Guo, Meina Qu, Hu Luo, Mei Han, Modeling and prediction of surface topography and surface roughness in dual-axis wheel polishing of optical glass, Int. J. Mach. Tool Manuf. 137 (2019) 13–29.
[9] Yaguo Li, Yongbo Wu, Libo Zhou, Masakazu Fujimoto, Vibration-assisted dry polishing of fused silica using a fixed-abrasive polisher, Int. J. Mach. Tool Manuf. 77 (2014) 93–102.
[10] M.-Y. Tsai, W.-Z. Yang, Combined ultrasonic vibration and chemical mechanical polishing of copper substrates, Int. J. Mach. Tool Manuf. 53 (2012) 69–76.
[11] H. Lee, H. Jeong, A wafer-scale material removal rate profile model for copper chemical mechanical planarization, Int. J. Mach. Tool Manuf. 51 (2011) 395–403.
[12] A.P. Abbott, G. Capper, K.J. McKenzie, K.S. Ryder, Voltammetric and impedance studies of the electropolishing of type 316 stainless steel in a choline chloride based ionic liquid, Electrochim. Acta 51 (2006) 4420–4425.
[13] D. Kim, K. Son, D. Sung, Y. Kim, W. Chung, Effect of added ethanol in ethylene glycol–NaCl electrolyte on titanium electropolishing, Corros. Sci. 98 (2015) 494–499.
[14] G.D. Kwona, Y.W. Kima, E. Moyena, D.H. Keuma, Y.H. Leea, S. Baik, D. Pribat, Controlled electropolishing of copper foils at elevated temperature, Appl. Surf. Sci. 307 (2014) 731–735.
[15] M. Sepúlveda, D. Quintero, J.G. Castaño, F. Echeverría, Improved two-step Brytal process for electropolishing of aluminum alloys, Corros. Sci. 136 (2018) 386–392.
[16] Fang Wang, Xinquan Zhang, H. Deng, A comprehensive study on electrochemical polishing of tungsten, Appl. Surf. Sci. 475 (2019) 587–597.
[17] W. Han, F. Fang, Fundamental aspects and recent developments in electropolishing, Int. J. Mach. Tool Manuf. 139 (2019) 1–23.
[18] G. Yang, B. Wang, K. Tawfiq, H. Wei, S. Zhou, G. Chen, Electropolishing of surfaces: theory and applications, Surf. Eng. 33 (2016) 149–166.
[19] H. Hocheng, P.S. Pa, Electropolishing of cylindrical workpiece of tool materials using disc-form electrodes, J. Mater. Process. Technol. 142 (2003) 203–212.
[20] G.L. Wynick, C.J. Boehlert, Use of electropolishing for enhanced metallic specimen preparation for electron backscatter diffraction analysis, Mater. Char. 55 (2005) 190–202.
[21] R. Rokicki, T. Hryniewicz, Enhanced oxidation–dissolution theory of electropolishing, Trans. IMF 90 (2013) 188–196.
[22] Piyushkumar B. Tailor, Amit Agrawal, S.S. Joshi, Evolution of electrochemical finishing processes through cross innovations and modeling, Int. J. Mach. Tool Manuf. 66 (2013) 15–36.
[23] T. Deng, J. Li, Z. Zheng, Fundamental aspects and recent developments in metal surface polishing with energy beam irradiation, Int. J. Mach. Tool Manuf. 148 (2020).
[24] S. Marimuthu, A. Triantaphyllou, M. Antar, D. Wimpenny, H. Morton, M. Beard, Laser polishing of selective laser melted components, Int. J. Mach. Tool Manuf. 95 (2015) 97–104.
[25] A. Kumar Singh, S. Jha, P.M. Pandey, Nanofinishing of a typical 3D ferromagnetic workpiece using ball end magnetorheological finishing process, Int. J. Mach. Tool Manuf. 63 (2012) 21–31.
[26] C.J. Wang, C.F. Cheung, L.T. Ho, M.Y. Liu, W.B. Lee, A novel multi-jet polishing process and tool for high-efficiency polishing, Int. J. Mach. Tool Manuf. 115 (2017) 60–73.
[27] M. Matlosz, S. Magaino, D. Landolt, Impedance analysis of a model mechanism for acceptor-limited electropolishing, J. Electrochem. Soc. 141 (1994) 410–418.
[28] R. Reizer, Simulation of 3D Gaussian surface topography, Wear 271 (2011) 539–543.
[29] Y.Z. Hu, K. Tonder, Simulation of 3-D random rough surface by 2-D digital filter and fourier analysis, Int. J. Mach. Tool Manuf. 32 (1992) 83–90.
[30] R. Christina Reggiani, F. Mazza, E. Sivieri, Electrochemical polishing of titanium in perchloric-methanolic solutions, Mater. Chem. 42 (1979) 149–158.
[31] T. Yanagishita, M. Imaizumi, T. Kondo, H. Masuda, Formation of porous Al particles by anisotropic anodic etching, Electrochem. Commun. 78 (2017) 26–28.
[32] M. Morinaga, 5-Titanium Alloys, Elsevier, 2019.
[33] C. Xia, Z. Feng, S. Liu, X. Zhang, B. Zhang, B. Pan, X. Zhang, M. Ma, R. Liu, Anisotropic pitting of single-phase β-Zr alloy and isotropic pitting of α + β double-phase Zr alloy, Corros. Sci. 127 (2017) 39–44.
[34] F.W. Ling, E.A. Starke, Thermal etching of β Ti-V alloys, Metallography 5 (1972) 399–407.
[35] D. Devilliers, J. Pouilleau, F. Garrido, S. Durand-Vidal, E. Mahe, Structure and composition of passive titanium oxide films, Mater. Sci. Eng., B 47 (1997) 235–243.
[36] L.Q. Guo, M.C. Lin, L.J. Qiao, Ferrite and austenite phase identification in duplex stainless steel using SPM techniques, Appl. Surf. Sci. 287 (2013) 499–501.
[37] C. Rotty, A. Mandroyan, M.-L. Doche, J.Y. Hihn, Electropolishing of CuZn brasses and 316L stainless steels: influence of alloy composition or preparation process (ALM vs. standard method), Surf. Coat. Technol. 307 (2016) 125–135.
[38] V. Vignal, H. Zhang, O. Delrue, O. Heintz, I. Popa, J. Peultier, Influence of long-term ageing in solution containing chloride ions on the passivity and the corrosion resistance of duplex stainless steels, Corros. Sci. 55 (2011) 894–903.
[39] S. Barison, S. Cattarin, S. Daolio, M. Musiani, A. Tuissi, Characterisation of surface oxidation of nickel–titanium alloy by ion-beam and electrochemical techniques, Electrochim. Acta 50 (2004) 11–18.
[40] A. Asserghine, M. Medvidović-Kosanović, L. Nagy, G. Nagy, In situ monitoring of the transpassivation and repassivation of the passive flm on nitinol biomaterial by scanning electrochemical microscopy, Electrochem. Commun. 107 (2019).
[41] S.A. Shabalovskaya, J.W. Anderegg, Surface spectroscopic characterization of TiNi nearly equiatomic shape memory alloys for implants, J. Vac. Sci. Technol. A 13 (1995) 2624–2632.